


Drag forces on nanoparticles in the free-molecule regime: Effect of the particle temperature

Jun Wang[✉],* Junjie Su, and Guodong Xia

Key Laboratory of Enhanced Heat Transfer and Energy Conservation, Ministry of Education, College of Environmental and Energy Engineering, Beijing University of Technology, Beijing 100124, People's Republic of China

 (Received 6 October 2019; revised manuscript received 5 December 2019; published 8 January 2020)

In the present paper, we theoretically study the drag force on nanoparticles in the free-molecule regime. It has been widely assumed that the particle temperature is equal to the gas media temperature in the open literature. However, this assumption can be invalid in some real applications. Based on the kinetic theory, we obtain the generalized formulas for the drag force on nanoparticles in the free-molecule regime. It is found that there exists a significant error induced by the assumption of equal temperature between the particle and the surrounding gas. Therefore, it is necessary to consider the effect of the particle temperature in the analysis of the particle transport properties.

DOI: [10.1103/PhysRevE.101.013103](https://doi.org/10.1103/PhysRevE.101.013103)

I. INTRODUCTION

Nanoparticles suspended in a gas can find applications in a wide range of fields, including combustion [1–3], biology [4,5], chemical engineering [6,7], micro- and nanoscale fabrication [8,9], and aerosol science [10]. An important issue is to predict the transport properties of nanoparticles, or even control the motion of nanoparticles. The transport of nanoparticles in a gas is dominated by the drag force. According to the Einstein relation [11], the diffusion coefficient of a suspended particle in a fluid is inversely proportional to the drag coefficient. This clearly necessitates a deep in-depth understanding of the drag force on nanoparticles in gas media.

Consider a nanoparticle with its characteristic size on the order of 10 nm. The mean free path of a gas in the standard state is about 100 nm, so the Knudsen number $\text{Kn} \gg 1$ and the transport of nanoparticles is in the free-molecule regime [12]. Here, $\text{Kn} = \lambda/L_c$, λ is the mean free path of the gas, and L_c is the characteristic size of the nanoparticle. In the free-molecule regime, the force exerted on the particle can be calculated based on the gas kinetic theory [13,14], i.e., by calculating the momentum transfer from the gas to the particle upon gas-particle collisions. Based on the assumption of rigid-body collisions between the gas molecules and the particle, Epstein obtained the formula of drag force [15],

$$\mathbf{F}_D = -\frac{8}{3}\delta\sqrt{2\pi m_g k_B T}NR^2\mathbf{V}. \quad (1)$$

Here, the parameter δ depends on the reflection scenario of the incident gas molecule. $\delta = 1$ and $\delta = (8 + \pi)/8$ refer to the two limiting cases of specular and diffuse scatterings [16], respectively. k_B is the Boltzmann constant. m_g , T , and N are the gas molecule mass, gas temperature, and number density of gas molecules, respectively. \mathbf{V} is the velocity of the suspended particle relative to the gas. Equation (1) can be used to predict the electric mobility of a microscale spherical

particle for large Kn [17]. However, as the particle size gradually decreases to the nanometer scale, the nonrigid-body interactions between the particle and gas molecules can play an important role in the gas-particle collision process and in turn the particle transport properties [18–23]. Experimental evidence includes the disagreement between the mobility sizes of nanoparticles measured by the differential mobility analyzer and those measured by the transmission electronic microscopy [24,25], the binary diffusion coefficient measurement of long-chain alkanes [26], and the size dependence of thermophoretic velocity in the nanoparticle deposition experiments [27]. It has been reported that the gas-particle nonrigid-body interactions cannot be neglected for nanoparticles with radius roughly smaller than 20–30 nm, depending on the temperature and the gas-particle interactions [16,28,29].

In the free-molecule regime, Li and Wang derived the generalized drag force for nanoparticles by taking into account the gas-particle nonrigid-body interactions [30],

$$\mathbf{F}_D = -\frac{8}{3}\sqrt{2\pi m_r k_B T}NR^2\Omega_{s/d}^{(1,1)*}\mathbf{V}, \quad (2)$$

where m_r is the reduced mass of the gas molecule and particle, $m_r = m_g m_p / (m_g + m_p)$; and m_p is the mass of the particle, $m_p \gg m_g$ in most cases. $\Omega_{s/d}^{(1,1)*}$ is the reduced collision integral, where the subscript “s/d” represents the cases of specular and diffuse scatterings, respectively. For rigid-body collisions, $\Omega_s^{(1,1)*} = 1$ and $\Omega_d^{(1,1)*} = (8 + \pi)/8$, so Eq. (2) turns out to be consistent with Eq. (1), and is a generalized expression.

It is worth noting that the theoretical analyses of the particle transport properties are usually on the basis of the assumption that the temperature of the particle T_p is equal to that of the surrounding gas T [15,30]. However, in some applications, the particle temperature is not equal to the media temperature ($T_p \neq T$), or even differs greatly. Examples include soot formation in the combustion process [3], fabrication of nanoparticles by vacuum evaporation [9], and heated nanoparticles by the photothermal effect [31]. Physically, the reflection of the gas molecules from the particle

*jwang@bjut.edu.cn

surface depends on the particle temperature and the gas-particle interaction [16,32]. For specular scatterings, the gas molecules are reflected elastically, so the influence of the particle temperature can be ignored. For diffuse scatterings, the impinging gas molecules are adsorbed on the particle surface and then reemitted in equilibrium with the particle surface [13,33], which significantly affects the momentum transfer between the particle and gas. The drag force on a nonuniformly heated spherical particle in a rarefied gas has been studied by considering the momentum and energy transfer between the particle and the surrounding gas for the whole range of Knudsen numbers [34]. In the free-molecule regime, Dahneke obtained the analytical formula for the drag force on a sphere body in the case of $T_p \neq T$ [35],

$$\mathbf{F}_s = -\frac{8}{3}\sqrt{2\pi m k_B T} N R^2 \mathbf{V}, \quad (3)$$

and

$$\mathbf{F}_d = -\frac{8 + \pi\sqrt{T_p/T}}{3}\sqrt{2\pi m k_B T} N R^2 \mathbf{V}, \quad (4)$$

for the specular and diffuse scatterings, respectively. Here, being similar to Eq. (1), Eqs. (3) and (4) are obtained based on the assumption of rigid-body collisions for the gas-particle interaction. For the nanosized particles in real applications, it is necessary to reconsider the drag in the case of $T_p \neq T$ by considering the gas-particle nonrigid-body interactions. For instance, the drag plays an important role for the estimation of the optical power spectral density in the optical tweezer technology owing to the collisions between the trapped nanoparticle and residual gas molecules [36–39]. This technology can be used for the cooling of trapped small particles from room temperature to quantum ground state (on the order of mK) [36,37], and for nanoscale temperature measurement by optical heating [38], wherein the gas-particle temperature difference has to be taken into account in the drag calculation.

In the present paper, we investigate the drag force on nanoparticles with $T_p \neq T$ in the free-molecule regime. The rest of the paper is organized as follows. In Sec. II, we derive the general expressions for the drag force on nanoparticles with $T_p \neq T$ in the free-molecule regime. In the rigid-body limit, the formulas are consistent with Eqs. (3) and (4). In Sec. III, the drag force on nanoparticles is evaluated by the Rudyak-Krasnolutski potential [40] as an example. The results for big particles are close to those for a rigid body, while the nonrigid-body effect is significant for small nanoparticles. The relative error owing to the assumption of $T_p = T$ could be larger than 50%, which necessitates an investigation on the effect of the particle temperature on the particle transport properties. Finally, we conclude the paper in Sec. IV.

II. DRAG FORCE ON NANOPARTICLES

In the present paper, nanoparticles are simplified as spheres, which are suspended in a diluted gas. The characteristic size of the particle L_c is equal to the radius of the sphere, R . In the free-molecule regime, the mean free path of gas molecules λ is much longer than R . Therefore, the influence

of the reflected gas molecules on the incoming molecules can be ignored, and it is reasonable to assume that the incident molecules strike the nanoparticle with a velocity distribution in uniform states, i.e., the Maxwell distribution. Based on the gas kinetic theory, the net force on the nanoparticle can be obtained by evaluating the momentum transfer during numerous collisions between the gas molecules and the particle.

The analytical model of the collision between a gas molecule and a nanoparticle is established in Fig. 1. \mathbf{v} and \mathbf{v}' represent the peculiar velocity of the gas molecule before and after collision. \mathbf{V} is the instantaneous velocity of the nanoparticle relative to the gas. For convenience, the coordinate system $\{x, y, z\}$ is established with its origin located at the body center of the particle, and z is the direction parallel to the direction of \mathbf{V} , as shown in Fig. 1. \mathbf{i} , \mathbf{j} , and \mathbf{k} represent the unit vectors of the x , y , and z directions, respectively. In the $\{x, y, z\}$ system, the velocities of the incoming gas molecule and reflected gas molecule are denoted by \mathbf{g} and \mathbf{g}' , respectively. Then, based on the theoretical framework given in Ref. [30], the drag force on a nanospherical particle in a diluted gas can be calculated by

$$\mathbf{F} = m_r \int_{\mathbf{v}} \mathbf{g} \mathbf{g}' f Q(\mathbf{g}) d\mathbf{v}. \quad (5)$$

Here, f is the velocity distribution of gas molecules [13,14],

$$f = \frac{N}{(2\pi k_B T/m_r)^{3/2}} \exp\left(-\frac{v^2}{2k_B T/m_r}\right), \quad (6)$$

and Q is the collision cross section upon the gas-particle collisions, which depends on the scattering scenario. Specular and diffuse scatterings are two limiting cases for the gas-particle collisions.

A. Specular scattering

For specular scatterings, the gas-particle collision is elastic, so the incident angle is equal to the scattering angle, and the momentum magnitude of the incident gas molecule is equal to that of the reflected gas molecule. The scattering angle is given by

$$\chi(\mathbf{g}, b) = \pi - 2b \int_{r_m}^{\infty} \left[r^2 \sqrt{1 - \frac{b^2}{r^2} - \frac{\Phi(r)}{m_r g^2/2}} \right]^{-1} dr, \quad (7)$$

where r is the separation distance, r_m is the closest distance that the gas molecules and particle could approach, b denotes the impact factor for the gas-particle collisions, and $\Phi(r)$ denotes the interaction potential between the gas molecule and the nanoparticle. The collision cross section for the specular case reads

$$Q_s(\mathbf{g}) = 2\pi \int_0^{\infty} (1 - \cos \chi) b db. \quad (8)$$

By substituting Eqs. (6)–(8) into Eq. (5), the drag force exerted on the nanoparticle can be obtained as

$$\mathbf{F}_s = -\frac{8}{3\pi} \sqrt{2\pi m_r k_B T} N \Omega_s^{(1,1)} \mathbf{V}. \quad (9)$$

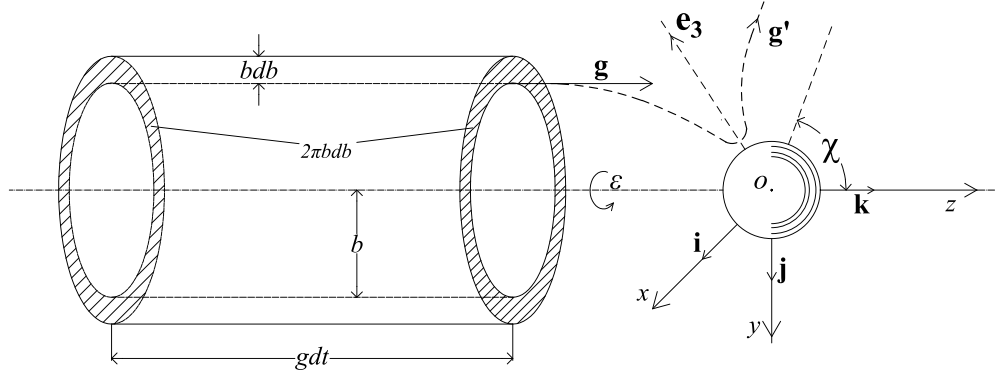


FIG. 1. The collision model of a nanoparticle with a gas molecule. b is the impact factor. χ denotes the scattering angle.

Here, the collision integral

$$\Omega_s^{(1,1)} = \int_0^\infty \exp(-\gamma^2) \gamma^5 Q_s(g) d\gamma, \quad (10)$$

with $\gamma = g/\sqrt{2k_B T/m_r}$. An reduced collision integral can be introduced:

$$\Omega_s^{(1,1)*} = \frac{\Omega_s^{(1,1)}}{\pi R^2}. \quad (11)$$

Then,

$$\mathbf{F}_s = -\frac{8}{3} \sqrt{2\pi m_r k_B T} N R^2 \Omega_s^{(1,1)*} \mathbf{V}. \quad (12)$$

For specular gas-particle scatterings, the gas molecule is reflected with the same magnitude of momentum as the incoming gas molecule. Therefore, there is no influence of the particle temperature on the resulting drag force on the nanoparticle in the case of the specular scattering limit.

B. Diffuse scattering

The diffuse scattering can be contributed to the gas molecule adsorption on the particle surface [41]. The adsorbed molecules walk randomly on the particle surface, and retain no memory about its incident momentum. Then, they are reflected from the particle surface in accordance with the Maxwell distribution at the particle surface temperature T_p ,

$$f' = c g f \exp\left(-\frac{g'^2}{2k_B T_p/m_r}\right), \quad (13)$$

where c is a constant and $g f$ denotes the incident mass flux. According to the conservation of molecules mass, $c = (m_r/k_B T_p)^2/2\pi$ and $g f = \int_{\mathbf{g}'} g' f' d\mathbf{g}'$.

In the case of diffuse gas-particle scatterings, the drag force on the nanoparticle is given by

$$\mathbf{F}_d = m_r \int_{\mathbf{v}} \mathbf{g} g f Q_d(g) d\mathbf{v}, \quad (14)$$

where the diffuse scattering cross section

$$Q_d(g) = 2\pi \left[\int_0^{b_0} \left(1 + \frac{1}{g} \sqrt{\frac{\pi k_B T_p}{2m_r}} \sin \frac{\chi}{2} \right) b db + \int_{b_0}^\infty (1 - \cos \chi) b db \right]. \quad (15)$$

Here, the impact factor b_0 refers to the orbiting scattering, by which the scattering angle χ goes to $-\infty$ [14]. For $b < b_0$, the gas molecules strike the nanoparticle in a diffuse manner, while for $b > b_0$, grazing collision takes place and the collision is specular. It should be noted that the diffuse scattering cross section $Q_d(g)$ depends on the particle temperature. By using $\gamma = g/\sqrt{2k_B T/m_r}$, $Q_d(g)$ can also be expressed as

$$Q_d(\gamma) = 2\pi \left[\int_0^{b_0} \left(1 + \frac{\sqrt{\pi}}{2\gamma} \sqrt{\alpha} \sin \frac{\chi}{2} \right) b db + \int_{b_0}^\infty (1 - \cos \chi) b db \right], \quad (16)$$

wherein α is a dimensionless temperature ratio, which is defined as $\alpha = T_p/T$. Putting Eq. (16) into Eq. (14) and integrating over g , the drag force is then rewritten as

$$\mathbf{F}_d = -\frac{8}{3\pi} \sqrt{2\pi m_r k_B T} N \mathbf{V} \int_0^\infty \gamma^5 e^{-\gamma^2} Q_d(g) d\gamma. \quad (17)$$

Similar to Eq. (11), the reduced collision integral in the diffuse scattering limit can be defined as

$$\Omega_{d,T_p}^{(1,1)*} = \frac{\int_0^\infty \gamma^5 e^{-\gamma^2} Q_d(g) d\gamma}{\pi R^2}. \quad (18)$$

Then, we have

$$\mathbf{F}_d = -\frac{8}{3} \sqrt{2\pi m_r k_B T} N R^2 \Omega_{d,T_p}^{(1,1)*} \mathbf{V}. \quad (19)$$

C. Parametrization

The specular and diffuse scatterings are two limit cases for the gas-particle collisions. A momentum accommodation factor (MAF) φ can be introduced to describe the gas-particle collision, which gives the percentage of gas molecules that are reflected from the particle surface in a diffuse manner. Then, a generalized expression for the drag force on a nanoparticle is written as

$$\mathbf{F}_D = -\frac{8}{3} \sqrt{2\pi m_r k_B T} N R^2 \Omega_{\text{avg}}^{(1,1)*} \mathbf{V}, \quad (20)$$

where the average reduced collision integral is given by

$$\Omega_{\text{avg}}^{(1,1)*} = \varphi \Omega_{d,T_p}^{(1,1)*} + (1 - \varphi) \Omega_s^{(1,1)*}. \quad (21)$$

Here, $\varphi = 0$ and $\varphi = 1$ correspond to the specular and diffuse scattering limits, respectively. It has been suggested that $\varphi \sim 0.9$ based on a lot of experimental data [42–44]. However, it is believed that the momentum accommodation factor decreases from 0.9 to 0 as the particle size decreases to a few nanometers. The transition depends on the temperature and the gas-particle interaction potentials [41,45].

D. Rigid-body collision limit

As the particle size increases, the gas-particle intermolecular interaction becomes less important and turns into a rigid-body collision. For a rigid sphere model, $\Omega_s^{(1,1)*} = 1$ and $\Omega_{d,T_p}^{(1,1)*} = [8 + \pi(T_p/T)^{1/2}]/8$, respectively. Then,

$$\mathbf{F}_{s,\text{rigid}} = -\frac{8}{3}\sqrt{2\pi m_r k_B T N R^2} \mathbf{V}, \quad (22)$$

and

$$\mathbf{F}_{d,\text{rigid}} = -\frac{8 + \pi\sqrt{T_p/T}}{3}\sqrt{2\pi m_r k_B T N R^2} \mathbf{V}, \quad (23)$$

which are consistent with Eqs. (3) and (4) [35]. Then, the parametrized expression can be given by

$$\mathbf{F}_{D,\text{rigid}} = -\frac{8 + \varphi\pi\sqrt{T_p/T}}{3}\sqrt{2\pi m_r k_B T N R^2} \mathbf{V}. \quad (24)$$

III. DRAG FORCE WITH RUDYAK-KRASNOLUTSKI POTENTIAL

As an example, the Rudyak-Krasnolutski (RK) potential can be employed to describe the interaction of a gas molecule with a particle, although it has limitations [46,47]. This potential model is constructed by the summation of the Lennard-Jones (LJ) interactions between the gas molecule and each constituent atom of the particle. The LJ potential is given by [48]

$$\Phi_{\text{LJ}}(r) = 4\varepsilon \left[\left(\frac{\sigma}{r} \right)^{12} - \left(\frac{\sigma}{r} \right)^6 \right], \quad (25)$$

where ε is the potential well depth, and σ is the collision diameter. The RK potential consists of a repulsive potential term $\Phi_9(r)$ and an attractive potential term $\Phi_3(r)$,

$$\Phi_{\text{RK}}(r) = \Phi_9(r) - \Phi_3(r). \quad (26)$$

Here,

$$\begin{aligned} \Phi_i(r) = & C_i \{ [(r-R)^{-i} - (r+R)^{-i}] \\ & - a_i [(r-R)^{-i+1} - (r+R)^{-i+1}] \}, \quad i = 3 \text{ or } 9, \end{aligned} \quad (27)$$

where, $a_3 = 3r/2$, $a_9 = 9r/8$, $C_3 = 2\pi\varepsilon\sigma^6/(3V)$, and $C_9 = 4\pi\varepsilon\sigma^{12}/(45V)$. The potential parameters for the interaction between the gas molecule and the constituent atom of the particle are given by the mixing rules, $\sigma = (\sigma_g + \sigma_p)/2$ and $\varepsilon = \sqrt{\varepsilon_g \varepsilon_p}$. Here the subscripts “g” and “p” denote the gas molecule and particle atom, respectively.

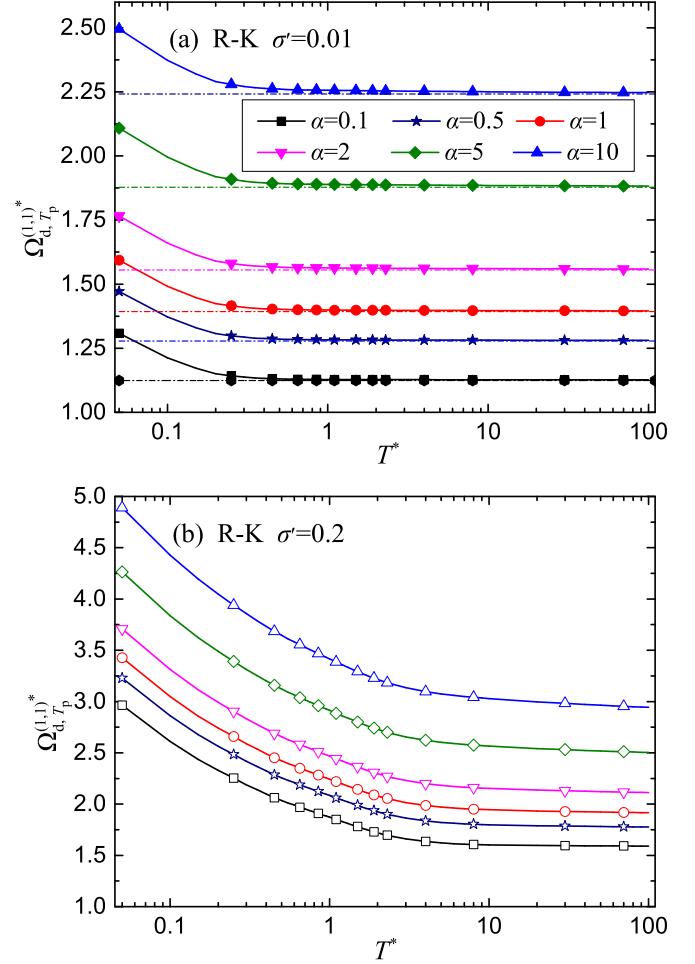


FIG. 2. $\Omega_{d,T_p}^{(1,1)*}$ versus T^* for the RK potential function with (a) $\sigma' = 0.01$ and (b) $\sigma' = 0.2$, respectively. The dotted lines denote the constant value of $(1 + \alpha^{1/2}\pi/8)$.

A. Drag force with constant MAF

Figure 2 presents the reduced collision integral $\Omega_{d,T_p}^{(1,1)*}$ as a function of the reduced temperature T^* for the RK potential. Here, $T^* = k_B T/\varepsilon$, $\alpha = T_p^*/T^*$, and $\sigma' = \sigma/R$. It can be seen that $\Omega_{d,T_p}^{(1,1)*}$ gradually decreases with increasing T^* . At high T^* , the gas molecules with large incoming momentum can easily overcome the potential barrier around the nanoparticle or be reflected from the particle in a short time, which results in a small collision section and a small collision integral as well. For a particle with very large radius ($\sigma' \rightarrow 0$), the collision between the gas molecule and nanoparticle tends to be rigid at high T^* . Therefore, the reduced collision integral in the case of $\sigma' = 0.01$ approaches the value for a rigid-body collision $(1 + \alpha^{1/2}\pi/8)$ at high T^* . With increasing σ' , the particle size decreases, and the effect of the gas-particle nonrigid-body collision is enhanced. Therefore, the reduced collision integral for high σ' is larger than that for low σ' . For diffuse scatterings, the incident molecules are reflected in a diffuse manner and therefore leave the surface in equilibrium with the particle at temperature T_p . If $T_p > T$, then the incident gas molecules are reflected with higher momentum, which in turn leads to an enhanced momentum transfer. If $T_p < T$,

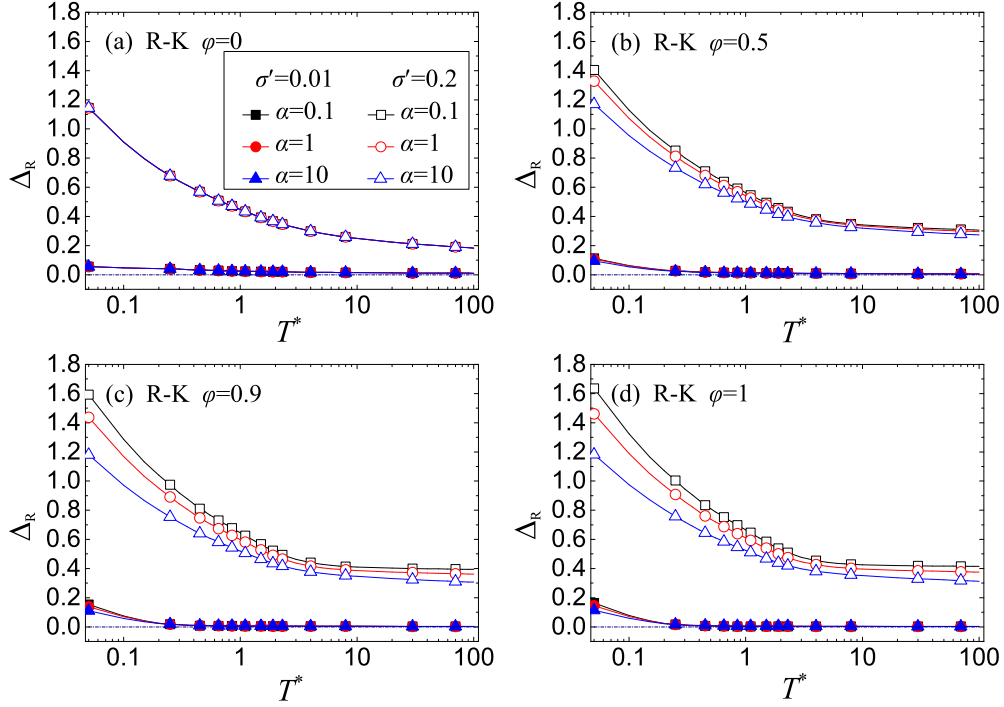


FIG. 3. Δ_R versus T^* for the RK potential function with $\sigma' = 0.01$ and $\sigma' = 0.2$. (a) $\varphi = 0$, (b) $\varphi = 0.5$, (c) $\varphi = 0.9$, and (d) $\varphi = 1$. Squares for $\alpha = 0.1$, circles for $\alpha = 1.0$, and triangles for $\alpha = 10.0$.

then the momentum transfer is suppressed. Therefore, $\Omega_{d,T_p}^{(1,1)*}$ increases with increasing α .

Figure 3 plots $\Delta_R = (\mathbf{F}_D/\mathbf{F}_{D,\text{rigid}}) - 1$ as a function of the reduced temperature T^* by using the RK potential with $\sigma' = 0.01$ and $\sigma' = 0.2$. Here, the momentum accommodation factor is assumed to be a constant for simplicity. In the case of $\sigma' = 0.01$, it is found that Δ_R is small in the whole temperature range and vanishes with increasing T^* . This is because the gas-particle interaction tends to be rigid for large particles, especially at high gas temperatures. Therefore, it is reasonable to neglect the gas-particle nonrigid-body interactions for large particles. As the particle radius decreases to a few nanometers, the particle size is comparable to the scale of the gas-particle intermolecular interactions. Then, the gas-particle nonrigid-body interactions cannot be ignored. In the case of $\sigma' = 0.2$, Δ_R could be much larger than 1, depending on the temperature and momentum accommodation factor. With increasing T^* , the effect of nonrigid-body collisions is suppressed, so Δ_R decreases. The value of Δ_R for high φ is larger than that for low φ because the effect of nonrigid-body interaction is very significant for diffuse scatterings.

The influence of the particle temperature on the momentum transfer between the particle and gas can be significant according to Figs. 2 and 3. Let $\Delta_T = (\mathbf{F}_D/\mathbf{F}_{D,T_p=T}) - 1$ be the relative error owing to the assumption of $T_p = T$. Here, $\mathbf{F}_{D,T_p=T}$ denotes the drag force under the assumption of $T_p = T$, wherein the gas-particle nonrigid-body interactions are taken into account. Figure 4 presents Δ_T as a function of T^* for the RK potential with $\sigma' = 0.01$ and $\sigma' = 0.2$. For $\varphi = 0$, the relative error $\Delta_T = 0$ ($\mathbf{F}_D = \mathbf{F}_{D,T_p=T}$) because the influence of the particle temperature cannot take effect in the limiting case of specular scattering, as shown in Fig. 4(a).

With increasing φ , the specular scattering turns into the diffuse scattering; then Δ_T becomes increasingly apparent. At low T^* , the influence of the temperature difference between the gas and particle is enhanced with increasing T^* for a given α , and Δ_T can be enlarged. As mentioned above, the gas-particle interaction tends to be rigid at high temperature in the case of $\sigma' = 0.01$. Therefore, Δ_T goes to the value for the limit of rigid-body collisions with varying T^* for $\sigma' = 0.01$; i.e., $\Delta_T = [\pi\varphi(\alpha^{0.5}-1)/(8+\pi\varphi)]$. However, in the case of $\sigma' = 0.2$ (small nanoparticles), the effect of the nonrigid body cannot be ignored. For very high T^* , Δ_T is almost a constant because the $\Omega_{d,T_p}^{(1,1)*}$ tends to be a constant.

B. Effect of the transition from specular to diffuse scattering

In Sec. III A, the momentum accommodation factor φ is assumed to be a constant for simplicity. However, based on the experimental and theoretical evidence, there is a transition from specular to diffuse scattering with increasing particle size [16,30,41,45,49]. For very small nanoparticles (with $R < 1$ nm), the gas-particle collision is dominated by the specular scattering [12,30]. For large particles with high Knudsen number, Millikan's experiments on oil drops suggest $\varphi \approx 0.9$ [42,43]. The transition is expected to occur at a particle radius of 2–3 nm [41,45]. In the present paper, the size dependence of the momentum accommodation factor is taken into account by introducing an empirical size-dependent momentum-accommodation function proposed in Ref. [16],

$$\varphi = \frac{1 + 0.9\text{Kn}\{1 - 1/[1 + (R/2.5)^{15}]\}}{1 + \text{Kn}}, \quad (28)$$

where R is in nanometers.

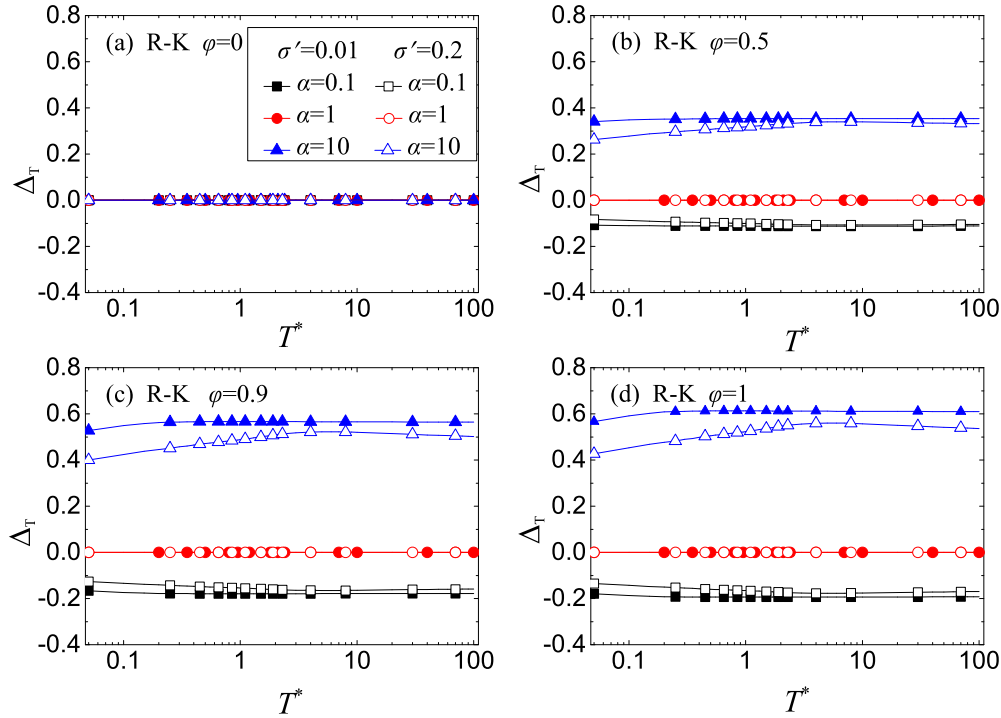


FIG. 4. Δ_T versus T^* for the RK potential function with $\sigma' = 0.01$ and $\sigma' = 0.2$. (a) $\phi = 0$, (b) $\phi = 0.5$, (c) $\phi = 0.9$, and (d) $\phi = 1$. Squares for $\alpha = 0.1$, circles for $\alpha = 1.0$, and triangles for $\alpha = 10.0$.

The drag force exerted on a silver nanoparticle suspended in He gas is calculated as an example. The LJ potential parameters are given as $\epsilon_{Ag} = 3995.4$ K, $\sigma_{Ag} = 2.574$ Å, and $\epsilon_{He} = 10$ K, $\sigma_{He} = 2.55$ Å. The parameters for the interaction potential between the gas molecule and the particle atom are given by the mixing rules given above. By using Eq. (28), Figure 5 plots the size dependence of Δ_R with $T^* = 1$. Therein, the Knudsen number is set as $Kn = 20$. As shown in Fig. 5, the relative error Δ_R goes down with increasing particle radius R . For very small R ($R < 2$ nm), it is found that the results for $\alpha = 0.1$, $\alpha = 1.0$, and $\alpha = 10.0$ are con-

sistent with each other. This is because the specular scattering dominates the gas-particle interactions for nanoparticles with radius $R < 2$ nm, and thus the influence of the particle temperature cannot take effect. The wavelike decrease of Δ_R in Fig. 5 is probably caused by the transition from specular to diffuse scattering. For $R > 10$ nm, Δ_R is less than 10%. With increasing particle size, the gas-particle nonrigid-body interactions become insignificant (Δ_R goes to 0) and the rigid-body collision assumption is applicable for $R > 30$ nm. Figure 6 presents Δ_T as a function of R . In the case of $\alpha = 1$ ($T_p = T$),

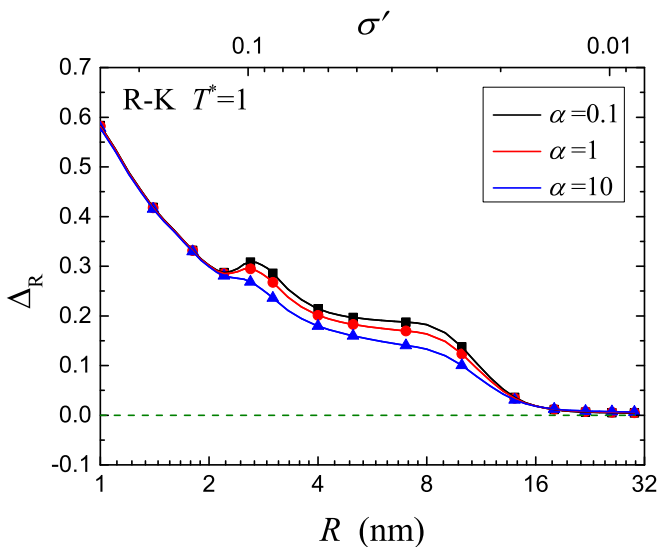


FIG. 5. Δ_R versus the particle radius R .

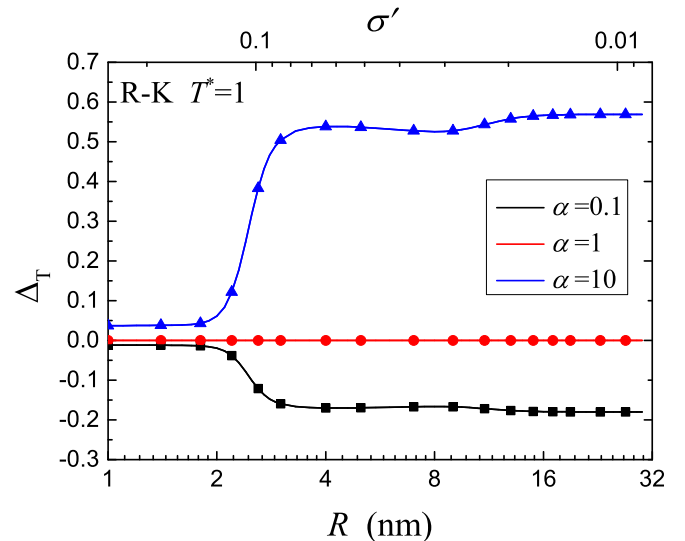


FIG. 6. Δ_T as a function of the particle radius R with different temperature ratio α .

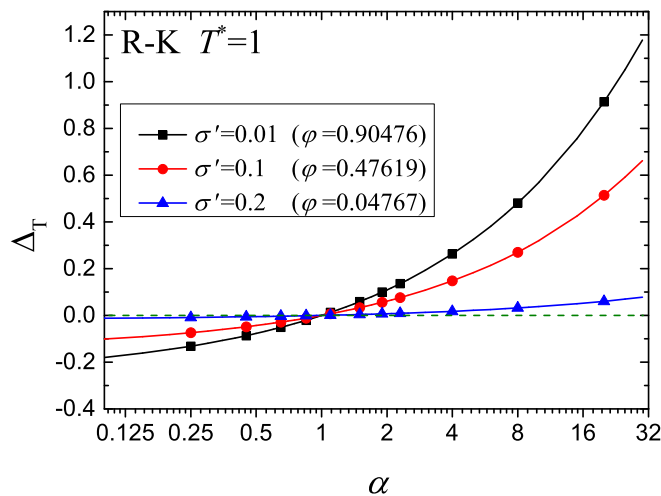


FIG. 7. Δ_T versus the temperature ratio α .

$\Delta_T = 0$ as it should. For a nanoparticle with $R < 2$ nm, as mentioned above, the dominant scattering mechanism is the specular reflecting, so $\Delta_T \approx 0$ and the influence of the particle temperature can be neglected in this case. The increase of the absolute value of Δ_T is quite abrupt in the range of $R = 2-3$ nm, where the transition from specular to diffuse scattering occurs. For larger particle size, the gas-particle collision is dominated by diffuse scatterings and the results are close to those in Fig. 4(c), where $\varphi = 0.9$.

According to Figs. 5 and 6, the error caused by the temperature difference between the gas and particle becomes significant when the temperature ratio α becomes large. Figure 7 plots Δ_T versus the temperature ratio α with $T^* = 1$. It is found that Δ_T vanishes for small particles ($\sigma' = 0.2$, $R = 1.281$ nm), as mentioned above. For the cases of $\sigma' = 0.1$ ($R = 2.562$ nm) and $\sigma' = 0.01$ ($R = 25.62$ nm), the relative

error owing to the gas-particle temperature difference, Δ_T increases significantly with the temperature ratio α . For $\sigma' = 0.1$, the absolute value of Δ_T is larger than 10% if $\alpha < 0.15$ or $\alpha > 2.5$, which can be considered as a significant error compared with the classical assumption of equilibrium gas-particle temperature. For $\sigma' = 0.01$, $\Delta_T > 10\%$ if $\alpha < 0.35$ or $\alpha > 1.9$.

IV. CONCLUSION

Based on the kinetic theory, the drag on nanoparticles is investigated in the free-molecule regime, wherein the gas-particle nonrigid-body interactions are taken into account. A general case is considered, by which the particle temperature T_p could be different from the gas media temperature T . The expressions for the drag force on nanoparticles are derived for both specular and diffuse scatterings, which are consistent with the expressions for the drag in the rigid-body limit. As an example, the Rudyak-Krasnolutski potential model of gas-particle interaction is employed to calculate the drag on nanoparticles. It is found that the relative error owing to the assumption of rigid-body collisions becomes insignificant with increasing particle size. The relative error owing to the assumption of $T_p = T$ could be larger than 50%, depending on the particle size and the temperature ratio T_p/T . For small nanoparticles with radius $R < 2$ nm, the error can be neglected because the specular scattering dominates the gas-particle interactions. After an abrupt increase of the error in the range of 2–3 nm, the effect of the particle temperature can be significant, especially for very large or small temperature ratios.

ACKNOWLEDGMENT

This work is supported by the National Natural Science Foundation of China (Grant No. 51776007).

- [1] V. Saxena, N. Kumarb, and V. K. Saxena, *Renewable Sustainable Energy Rev.* **70**, 563 (2017).
- [2] R. A. Yetter, G. A. Risha, and S. F. Son, *Proc. Combust. Inst.* **32**, 1819 (2009).
- [3] M. Koegl, B. Hofbeck, S. Will, and L. Zigan, *Appl. Energy* **209**, 426 (2018).
- [4] D. Westmeiera, D. Solouk-Saranb, and C. Vallet, *Proc. Natl. Acad. Sci. U.S.A.* **115**, 7087 (2018).
- [5] Q. A. Pankhurst, S. K. Jones, and J. Dobson, *J. Phys. D: Appl. Phys.* **49**, 501002 (2016).
- [6] A. J. M. Mackus, M. J. Weber, and N. F. W. Thissen, *Nanotechnology* **27**, 034001 (2015).
- [7] S. Linic, U. Aslam, and C. Boerigter, *Nat. Mater.* **14**, 567 (2015).
- [8] J. Qiu and T. Qiu, *Carbon* **81**, 20 (2015).
- [9] N. Rajput, *Int. J. Adv. Eng. Technol.* **7**, 1806 (2015).
- [10] R. Givehchi and Z. Tan, *J. Aerosol Sci.* **83**, 12 (2015).
- [11] A. Einstein, *Ann. Phys. (Leipzig)* **17**, 549 (1905).
- [12] H. Tsien, *J. Aeronaut. Sci.* **13**, 653 (1946).
- [13] S. Chapman and T. G. Cowling, *The Mathematical Theory of Non-Uniform Gases* (Cambridge University Press, Cambridge, UK, 1970).
- [14] J. O. Hirschfelder, C. F. Curtiss, and R. B. Bird, *Molecular Theory of Gases and Liquids* (Wiley, New York, 1954).
- [15] P. S. Epstein, *Phys. Rev.* **23**, 710 (1924).
- [16] Z. Li and H. Wang, *Phys. Rev. E* **68**, 061207 (2003).
- [17] M. Li, G. W. Mulholland, and M. R. Zachariah, *Aerosol Sci. Technol.* **46**, 1035 (2012).
- [18] M. Zurita-Gotor, *J. Aerosol. Sci.* **37**, 283 (2006).
- [19] J. Wang and Z. Li, *Phys. Rev. E* **84**, 021201 (2011).
- [20] J. Wang, S. Luo, and G. Xia, *Phys. Rev. E* **95**, 033101 (2017).
- [21] S. Luo, J. Wang, G. Xia, and Z. Li, *J. Fluid Mech.* **809**, 345 (2016).
- [22] L. Mädler and S. K. Friedlander, *Aerosol Air Qual. Res.* **7**, 304 (2007).
- [23] M. Li, G. W. Mulholland, and M. R. Zachariah, *Phys. Rev. E* **89**, 022112 (2014).
- [24] H. G. Scheibel and J. Porstendörfer, *J. Aerosol Sci.* **14**, 113 (1983).
- [25] Y. Kuga, K. Okauchi, D. Takeda, Y. Ohira, and K. Ando, *J. Nanopart. Res.* **3**, 175 (2001).
- [26] C. Liu, R. Zhao, R. Xu, F. N. Egeolfopoulos, and H. Wang, *Proc. Combust. Inst.* **36**, 1523 (2017).

- [27] Y. Zhang, S. Li, W. Yan, and Q. Yao, *Powder Technol.* **227**, 24 (2012).
- [28] L. G. Longsworth, *J. Am. Chem. Soc.* **74**, 4155 (1952).
- [29] Z. Li, *Phys. Rev. E* **80**, 061204 (2009).
- [30] Z. Li and H. Wang, *Phys. Rev. E* **68**, 061206 (2003).
- [31] Z. Wang, C. Yang, and F. Huang, *Energy Environ. Sci.* **6**, 3007 (2013).
- [32] J. Wang and Z. Li, *Phys. Rev. E* **86**, 011201 (2012).
- [33] S. Yu, J. Wang, G. Xia, and L. Zong, *Phys. Rev. E* **97**, 053106 (2018).
- [34] S. A. Beresnev, V. G. Chernyak, and G. A. Fomyagin, *J. Fluid Mech.* **219**, 405 (1990).
- [35] B. E. Dahneke, *J. Aerosol Sci.* **4**, 147 (1973).
- [36] T. Li, S. Kheifets, and M. G. Raizen, *Nat. Phys.* **7**, 527 (2011).
- [37] J. Gieseler, B. Deutsch, R. Quidant, and L. Novotny, *Phys. Rev. Lett.* **109**, 103603 (2012).
- [38] J. Millen, T. Deesuwana, P. Barker, and J. Anders, *Nat. Nanotechnol.* **9**, 425 (2014).
- [39] Y. Amarouchene, M. Mangeat, B. V. Montes, L. Ondic, T. Guérin, D. S. Dean, and Y. Louyer, *Phys. Rev. Lett.* **122**, 183901 (2019).
- [40] V. Ya. Rudyak and S. L. Krasnolutski, *Dokl. Phys.* **46**, 897 (2001).
- [41] C. Liu and H. Wang, *Phys. Rev. E* **99**, 042127 (2019).
- [42] R. A. Millikan, *Phys. Rev.* **22**, 1 (1923).
- [43] R. A. Millikan, *Phys. Rev.* **21**, 217 (1923).
- [44] M. D. Allen and O. G. Raabe, *J. Aerosol. Sci.* **13**, 537 (1982).
- [45] Z. Li and H. Wang, *Phys. Rev. Lett.* **95**, 014502 (2005).
- [46] L. A. Girifalco, M. Hodak, and R. S. Lee, *Phys. Rev. B* **62**, 13104 (2000).
- [47] R. Y. M. Wong, C. Liu, and J. Wang, *J. Nanosci. Nanotechnol.* **12**, 2311 (2012).
- [48] J. K. Johnson, J. A. Zollweg, and K. E. Gubbins, *Mol. Phys.* **78**, 591 (1993).
- [49] J. F. de la Mora, L. de Juan, K. Liedtke, and A. Schmidt-Ott, *J. Aerosol Sci.* **34**, 79 (2003).